The Wavepacket Motion via a Conical Intersection in Photochemistry of Aqueous Transition Metal Dianions

ARTICLE *in* JOURNAL OF PHYSICAL CHEMISTRY LETTERS · MAY 2011

Impact Factor: 7.46 · DOI: 10.1021/jz200239b

3 AUTHORS, INCLUDING:

Mikhail N Ryazantsev
Emory University
17 PUBLICATIONS **199** CITATIONS
SEE PROFILE

Alexander Tarnovsky
Bowling Green State University
74 PUBLICATIONS **965** CITATIONS
SEE PROFILE

THE JOURNAL OF PHYSICAL CHEMISTRY Letters

LETTER

pubs.acs.org/JPCL

Wavepacket Motion via a Conical Intersection in the Photochemistry of Aqueous Transition-Metal Dianions

Igor L. Zheldakov,[†] Mikhail N. Ryazantsev,[‡] and Alexander N. Tarnovsky*

Department of Chemistry and Center for Photochemical Sciences, Bowling Green State University, Bowling Green 43403, Ohio, United States

Supporting Information

ABSTRACT: The photochemical reaction paths in aqueous $PtBr_6^{2-}$ and $OsBr_6^{2-}$ have been studied by femtosecond broad-band pump−probe spectroscopy supported by CASPT2 and DFT/TDDFT calculations. These paths lead to the separation of negative charges and propagate through distortions of nascent, penta-coordinated metal fragments caused by Jahn−Teller C_{4v} and D_{3h} conical intersections (CIs), respectively. Within 150 fs following 420 nm excitation of $PtBr_6^{2-}$, the molecule undergoes internal conversion and intersystem crossing into the dissociative lowest triplet excited $^3T_{1g}$ state, loses a ligand, and relaxes via the C_{4v} CI to the nearly trigonal bipyramid $^3PtBr_5^-$ product in the triplet state. Direct 530 nm excitation of $PtBr_6^{2-}$ to $^3T_{1g}$ yields the same product. Oscillations observed in the bending and umbrella a_1 modes of $^3PtBr_5^-$ arise from impulsive excitation of, respectively, one of the reaction coordinate modes, which is parallel to the gradient difference vector of the C_{4v} CI, and the "spectator" mode that preserves the electronic degeneracy.

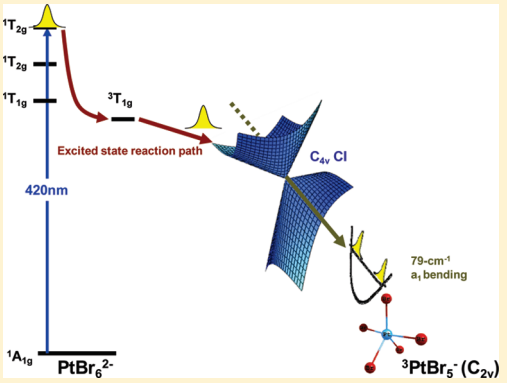

SECTION: Dynamics, Clusters, Excited States

Transition-metal compounds are actively integrated into schemes for solar energy conversion, photocatalysis, and photovoltaics. In these applications, the population optically delivered to the Franck−Condon region of the initial excited electronic state often travels over several potential energy surfaces (PESs) before arriving to a product state with useful functions. Radiationless relaxation between multidimensional PESs of polyatomic molecules takes place through avoided crossings[1] or, more typically, through real crossings — conical intersections (CIs).[2−4] The forces driving the radiationless relaxation are attracting considerable interest, and ultrafast laser experiments made it possible to monitor the wavepacket motion in real time.[5−8] The role of CIs in photochemical reactions continues to be tested more stringently in experiments.[9−14]

Coherent vibrational motion in products of photodissociation reactions has been previously observed.[5,9,10,12] Impulsive excitation of a reactant such that the pulse bandwidth is sufficiently broad to excite several vibrational states, creates a wavepacket — coherent superposition of energy eigenstates on the excited PES. The relevant modes and "spectator" modes orthogonal to the reaction coordinate may become impulsively excited and transfer their coherence to the product modes.[15] A vibrational wavepacket in the product state may also be formed via bond breaking when an impulsive force is imparted to the nuclear coordinates coupled to the dissociation reaction coordinate. Vibrational coherences have also been associated with the passage of a molecule through a CI[9,11−13] and attributed to a sudden change of the force field at the intersection, analogous to impulsive bond breaking.[10−12] The Jahn−Teller (JT) theorem states that a nonlinear molecule in a degenerate electronic state is distorted by suitable nontotally symmetric vibrations with the concomitant stabilization of energy.[4] A degenerate electronic E state at C_{4v} or D_{3h} geometries represents JT C_{4v} CI or JT D_{3h} CI and has its degeneracy split by vibrations of b_1 and b_2 symmetry or e symmetry, respectively.[3,4] The gradient difference and derivative coupling vectors are linear combinations of the splitting normal modes; these vectors define the CI "branching plane" and form a "moat" of the JT CI on the lower adiabatic surface. JT relaxation has been a subject of time-resolved studies, notably, in the CO ligand loss from gas-phase $Cr(CO)_6$, where the propagation of the ^1E state $Cr(CO)_5$ wavepacket through a JT D_{3h} CI excites a coherent bending motion detected in $^1S_0$ $Cr(CO)_5$.[9,10,12]

We report on photoproduct coherence in water and methanol solutions of transition metal complexes with the structural formula MBr_6^{2-} (M = Pt, Os). The O_h structure of $PtBr_6^{2-}$ is defined by d^6 electrons fully occupying the t_{2g} orbital set. The unequal occupation of the t_{2g} orbital set by d^4 electrons in $OsBr_6^{2-}$ distorts its geometry to D_{4h}. Excitation at 420 and

Received: February 22, 2011
Accepted: May 23, 2011
Published: May 23, 2011

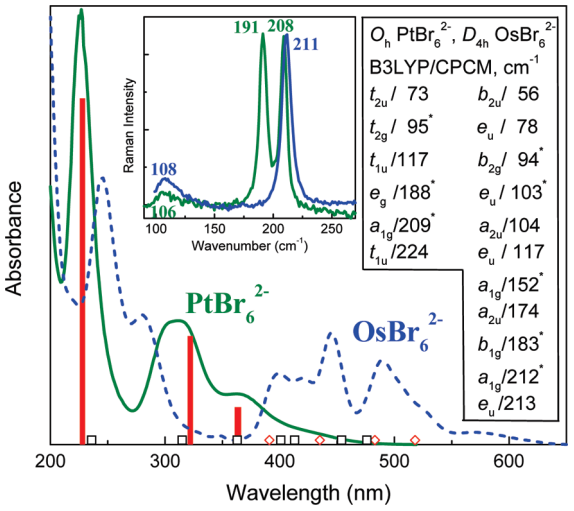

Figure 1. UV−vis of aqueous $PtBr_6^{2-}$ and $OsBr_6^{2-}$ (absorption cross sections at 420 nm and 8.77×10^{-18} and 2.07×10^{-17} cm^2, respectively). We report CASPT2 VETs in $PtBr_6^{2-}$ (CAS(22,13)/full ANO-RCC, MOLCAS 7.4, constrained to D_{2h} symmetry), where allowed transitions are shown as red bars of the lengths proportional to the calculated oscillator strengths, whereas squares and diamonds indicate forbidden transitions to singlet and triplet states. At energies comparable or less than the 420 nm photon energy, three singlet and three triplet excited states are predicted, $^1T_{1g}$ LF (476 nm), mixed LF/CT $^1T_{2g}$ (454 nm) and $^1T_{2g}$ (413 nm), and $^3T_{1g}$ LF (518 nm), $^3T_{2g}$ LF (483 nm), and $^3T_{1u}$ CT (435 nm). The inset shows the Raman spectra of 30 mM solutions (785 nm excitation). B3LYP/CPCM frequencies of aqueous $PtBr_6^{2-}$ and $OsBr_6^{2-}$ scaled by a factor of 1.10 (listed, Raman-active vibrations are indicated by an asterisk) are in agreement with those observed in the Raman spectra within 3.5 cm^{-1}, and consequently, this method was used for product frequency calculations.

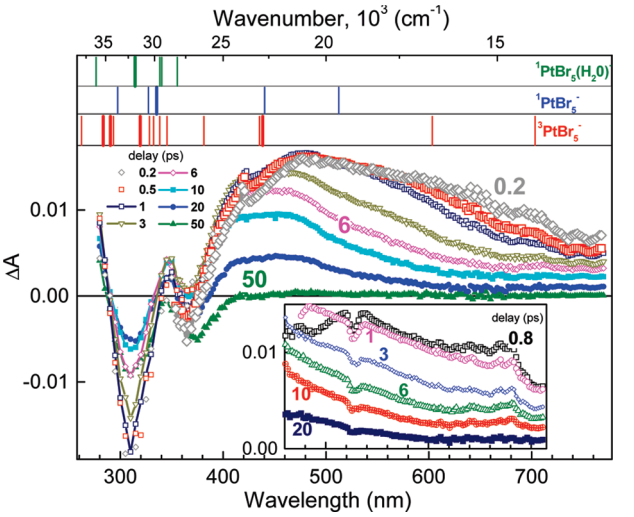

Figure 2. 420 nm ΔA spectra of aqueous $PtBr_6^{2-}$ (3.5 mM) flowed through a 0.3 mm jet. Bottom inset: 530 nm ΔA spectra. Top insets: the M052X VETs of possible products with oscillator strengths larger (thick lines) and smaller (thin lines) than 0.01.

530 nm carried out in this work promotes $PtBr_6^{2-}$ ($^1A_{1g}$) to the mixed ligand-field/charge-transfer (LF/CT) singlet $^1T_{2g}$ state (413 nm) and the lowest excited triplet $^3T_{1g}$ LF state[16] (518 nm) and $OsBr_6^{2-}$ ($^3A_{1g}$) to one of the ligand-to-metal CT (LMCT) states (~420 nm), Figure 1. The sole reaction caused by irradiation of aqueous $PtBr_6^{2-}$ in the 313−530 nm range is aquation that leads to a primary $PtBr_5(H_2O)^-$ product via heterolytic Pt−Br bond cleavage.[17]

For $PtBr_6^{2-}$, our CASPT2 vertical electronic transitions (VETs) reproduce its experimental spectrum and are in excellent agreement with TDDFT calculations of VETs using the M052X density functional with the Def2-TZVP (Pt) and aug-cc-pVTZ-PP (Br) basis sets (Gaussian 09). The latter method, which is less computationally expensive, in combination with a conductor-like polarizable continuum model (CPCM) was employed for VET calculations of possible ground-state products, $^1PtBr_5^-$, $^3PtBr_5^-$, and $^1PtBr_5(H_2O)^-$. At the M052X level, $^3PtBr_5^-$ has a C_{2v} geometry with $\angle Br_{ax}PtBr_{eq}$ = 90 and 109° and $\angle Br_{eq}PtBr_{eq}$ = 90 and 142°, resembling a D_{3h} trigonal bipyramid (quasi-TBP), see Supporting Information. This species is 2.21 eV above $^1A_{1g}$ $PtBr_6^{2-}$, and 1.1 eV above the $^1PtBr_5^-$ with a C_{4v} square-based pyramid (SP) geometry. Ground-state $^3OsBr_5^-$ and $^1OsBr_5^-$ are near-SP ($\angle Br_{ax}PtBr_{eq}$ = 96.6°, $\angle Br_{eq}PtBr_{eq}$ = 90°) and TBP, respectively, lying 1.08 and 1.51 eV above $^3A_{1g}$ $OsBr_6^{2-}$. The M052X energy minimum optimization of the $^3T_{1g}$ LF state in $PtBr_6^{2-}$ starting from the Franck−Condon point revealed a dissociative surface along the Pt−Br reaction coordinate, as expected.[18,19]

In our transient absorption setup,[20] two TOPAS-C optical parametric amplifiers generated 420 or 530 nm pump pulses with the energy of 2 μJ (spot size, 300 μm) and probe pulses tunable between 270 and 400 nm. A white-light continuum probe was used from 340 to 770 nm. The pump−probe cross-correlation (CCF) was 150 fs (fwhm). The pump and probe beam polarizations were set at the magic angle (54.7°) for transient absorption spectra or the parallel (∥) and perpendicular (⊥) angles for 420 nm pump/730 nm probe anisotropy. All data were corrected for the chirp of the probe beam.[20]

The results following 420 nm excitation of aqueous $PtBr_6^{2-}$, which is predominantly to the 413 nm $^1T_{2g}$ LF/CT state, are summarized below.

(i) The early time transient absorption (ΔA) covers the range from 370 to 770 nm with the maximum at ~500 nm (time delay, $\Delta\tau$ = 100 fs), where it exhibits a sub-200 fs rise attributed to the photoproduct formation, Figures 2 and 3. An unambiguous marker for time zero, $\Delta\tau$ = 0, is provided by the solvent cross-phase modulation signals, Figure 3.

(ii) Two different types of damped coherent oscillations are observed. (a) Modulations with a fast Fourier transform (FFT) frequency of ~209 cm^{-1} are present only within the ground-state absorption of $PtBr_6^{2-}$, Figure 3D−F. The origin of these oscillations must be associated with the resonance impulsive stimulated Raman scattering (RISRS) from ground-state $PtBr_6^{2-}$ because the corresponding vibrational frequency is observed in the conventional Raman spectrum, Figure 1. (b) The 78 ± 10 cm^{-1} FFT band that appears as a shoulder of the strong 113 ± 3 cm^{-1} FFT band, and in comparison, shows some anharmonicity changing from 78 to 84 cm^{-1} with increasing probe energy. These oscillations have solvent-independent frequencies and are weak near the center but strong at the blue and red wings of the 500 nm photoproduct band. The ΔA(∥) and ΔA(⊥) signals show the same beat amplitude.

(iii) A time constant of τ_1 = 150 ± 30 fs for the photoproduct formation is obtained by multiexponential deconvolution of the ΔA kinetic traces measured in the 500 nm region, where the oscillations are not pronounced. Narrowing and blue shifting of

dx.doi.org/10.1021/jz200239b | J. Phys. Chem. Lett. 2011, 2, 1540–1545

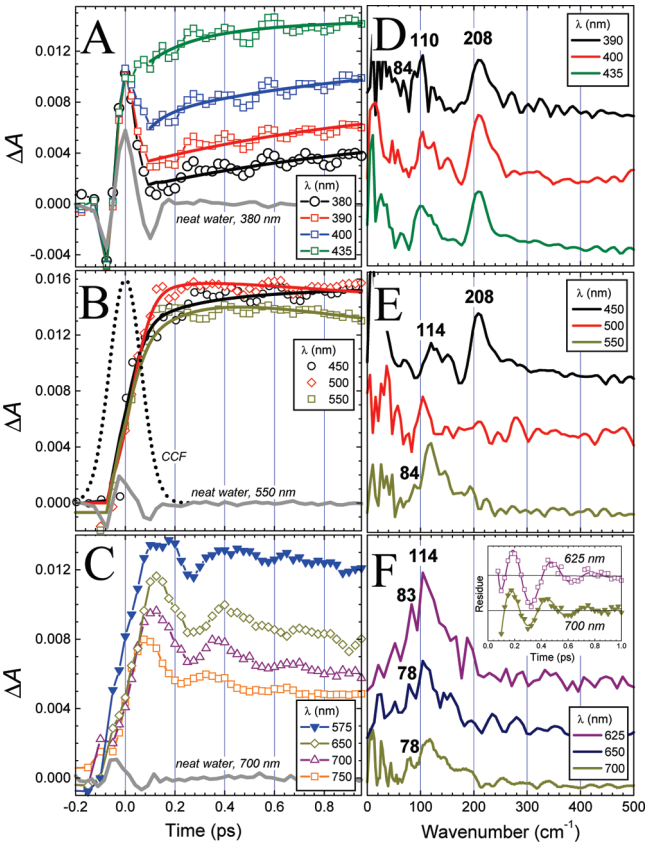

Figure 3. (A−C) Early time ΔA kinetic traces (symbols) from the spectra of aqueous $PtBr_6^{2-}$ in Figure 2 and signals (gray lines) from water. The solid lines are multiexponential fits, convoluted with a CCF function in B, not shown in C. (D−F) FFT analysis and fits to eq 1 (F, inset) of the residuals.

the product 500 nm band ($\tau_2 \approx 600$ fs) is followed by its decay and rise of the broad 430 nm band ($\tau_3 \approx 1.6$ ps). This band undergoes biphasic decay with $\tau_4 \approx 7$ ps and $\tau_5 \approx 15$ ps accompanied by partial recovery of ground-state bleach.

(iv) The ΔA spectra (Figure 2, inset) and product coherences upon 530 nm excitation directly to the $^3T_{1g}$ state are identical to those upon 420 nm excitation to the $^1T_{2g}$ state.

(v) The amplitudes (A), frequencies (ν), phase shifts (ϕ, $-\phi/2\pi\nu$ is equal to a temporal onset), and decay time constants (τ_c) of the oscillatory components are obtained by subtracting the multiexponential fits from the measured ΔA kinetics and fitting the residue $R(t)$ to a sum of two damped cosine functions

$$R(t) = \sum_{i=1,2} A_i \cdot \exp(-t/\tau_{ci}) \cdot \cos(2\pi\nu_i t + \phi_i) \qquad (1)$$

The derived frequencies agree with those obtained by FFT. In the photoproduct, the $\nu_1 \approx 113$ cm^{-1} has $\tau_{c1} = 235 \pm 50$ fs and an almost zero temporal onset of -7 ± 8 fs, whereas the $\nu_2 \approx 74$ cm^{-1} is characterized by a noticeable onset of 30 ± 35 fs and is short-lived, $\tau_{c2} = \sim 75$ fs. The inclusion of the 74 cm^{-1} component in the fit is necessary as it cancels out the first kick of the 113 cm^{-1} oscillation to make the subsequent kick more pronounced, for example, the trough in the inset of Figure 3F. The 113 cm^{-1} oscillation, as well as the oscillation at ~74 cm^{-1}, exhibits a π-phase shift in the blue and red wings of the 500 nm photoproduct band. Oscillations due to RISRS show $\tau_{c3} = 1.4 \pm 0.4$ ps and a temporal onset of -33 ± 18 fs, corresponding to the phase near $3\pi/2$.

Following 420 nm excitation of aqueous $OsBr_6^{2-}$, we observed (a) modulations with a solvent-independent frequency $\nu_1 = 208 \pm 2$ cm^{-1}, a ~30 fs time lag, persisting to long times, $\tau_{c1} = 1.33 \pm 0.12$ ps. They are weak near the center but pronounced in the wings of two 540 and 675 nm product bands. The π-phase jump is clearly observed within the 675 nm band. The oscillations show small anisotropy ($r \leq 0.04$). (b) RISRS oscillations from 340 to 475 nm within ground-state absorption of $OsBr_6^{2-}$, with the isolated 108 cm^{-1} frequency ($\tau_{c2} = 250$ fs) and two overlapping 156 and 178 cm^{-1} bands matching those in the Raman spectrum (computed 152 and 183 cm^{-1} modes are weak in the experimental spectrum). In the fit of the data to eq 1, the latter RISRS bands are not resolvable and are described as a single component with $\tau_{c3} = 319$ fs, the value of which is determined along with τ_{c2} at 430 and 530 nm, where the amplitude of the ν_1 component is 0.

RISRS oscillations occur due to excitation of fundamental vibrational modes of the ground-state parent dianion whose frequencies fall within the laser spectral bandwidth. This phenomenon is well understood. The RISRS damping times agree with those derived from Raman bandwidths in Figure 1, and the spectral dependence of the RISRS amplitude is as reported.[21,22]

Following 420 nm excitation of aqueous $PtBr_6^{2-}$, the delayed rise of the transient absorption ($\tau_1 = 150$ fs) rules out its interpretation as absorption from the initially excited $^1T_{2g}$ state because its rise should be instrument-limited. Moreover, the early time transient absorption is similar to that observed following 530 nm excitation directly into the lowest excited $^3T_{1g}$ state, which also rules out absorption from higher-lying $^3T_{2g}$, $^3T_{1u}$ triplet and $^1T_{1g}$, $^1T_{2g}$ singlet states. Spectral evolution due to vibrational relaxation is predictable,[23] and that observed is inconsistent with hot $^1A_1$ $PtBr_6^{2-}$. The lowest $^3T_{1g}$ LF state is dissociative. Therefore, the early time transient absorption is assigned to the ground-state quasi-TBP $^3PtBr_5^-$, in agreement with its intense transitions in the red region, Figure 2. This species undergoes vibrational relaxation and solvation (τ_2) and then intersystem crossing (τ_3) to the ground-state SP $^1PtBr_5^-$ (430 nm band), which undergoes geminate recombination (τ_4) and aquation (τ_5) to form $^1PtBr_5(H_2O)^-$. Ligand substitution in $PtBr_6^{2-}$ and $OsBr_6^{2-}$ will be discussed separately.

Relaxation via close-lying electronic states and intersystem crossing (ISC) processes following the promotion of $PtBr_6^{2-}$ into the $^1T_{2g}$ state leads to the same dissociative $^3T_{1g}$ LF state directly populated at 530 nm. Theoretically, a spin−orbit interaction is turned on as a molecule passes along a suitable vibrational coordinate through a crossing of the singlet and triplet surfaces. Sub-20 fs ISC from initially prepared ^{1}MLCT to ^{3}MLCT in solvated $Fe(bpy)_3$ has been interpreted as resulting from surface crossing via a single oscillation of a high-frequency 1607 cm^{-1} mode associated with the ligand deformation.[24] In $PtBr_6^{2-}$, t_{1u} and t_{2u} modes that would mediate ISC from $^1T_{2g}$ to close-lying $^3T_{1u}$ are Raman-inactive. Therefore, relaxation will likely occur via a manifold of singlet states to $^1T_{1g}$. ISC from the $^1T_{1g}$ surface to the $^3T_{2g}$ and $^3T_{1g}$ surfaces is mediated by Raman-active t_{2g}, e_g, and a_{1g} modes ($^1T_{1g} \otimes T_{2g}$ (e_g, a_{1g}) $\supset$ $^3T_{1g}$, $^3T_{2g}$) and takes less than a period of the fastest a_{1g} mode (208 cm^{-1}), as inferred from the 150 fs formation of $^3PtBr_5^-$. If ISC occurs to $^3T_{2g}$, a molecule should rapidly populate $^3T_{1g}$ based on a small energy gap and dissociate.

Next, let us discuss mechanisms that may give rise to the beats in product absorption. The ratio of the modulated to unmodulated

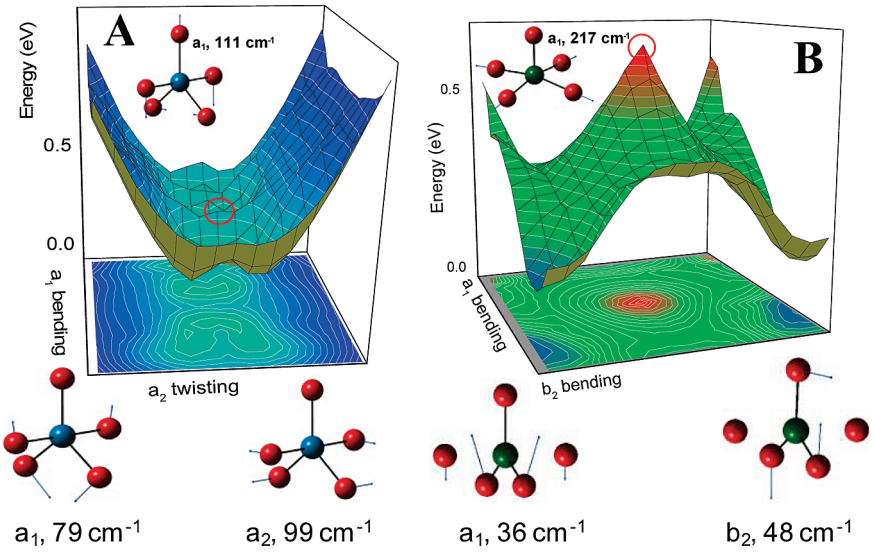

Figure 4. M052X scans of ground-state PESs of $^3PtBr_5^-$ (A) and $^3OsBr_5^-$ (B) along the "branching space" coordinates. Open circles schematically show CI locations. Insets: a_1 vibrations impulsive excited via metal−ligand bond breaking.

ΔA signals is ∼55% for $PtBr_6^{2-}$. Electronic coherence is known to manifest itself as beats of large amplitude. The beat amplitude changes with a wavelength similar to the product band.[25,26] This is also observed in a stepwise population transfer from a precursor state to a product state through avoided crossing.[7] The energy gap between close-lying electronic states, and therefore, the wavepacket oscillation frequency, is sensitive to solvent polarity.[25] Also, electronic beats show large anisotropy of transition moment directions of the coupled electronic states.[27,28] However, this is not what we observed. The π-phase shift observed suggests coherent vibrational motion on the product PES.[5−8] In $^3PtBr_5^-$, the 113 cm^{-1} oscillation is in the a_1 umbrella (111 cm^{-1}, B3LYP), whereas the 78 cm^{-1} frequency matches the a_1 bending (79 cm^{-1}, B3LYP), Figure 4. On the basis of the 208 cm^{-1} frequency observed, the a_1 stretch (217 cm^{-1}, B3LYP) is excited in SP $^3OsBr_5^-$, which absorbs in the 540 and 675 nm bands.

Impulsive excitation of $PtBr_6^{2-}$ and $OsBr_6^{2-}$ creates vibrational wavepackets in the Franck−Condon state. We attribute the a_1 modes (113 cm^{-1} in $^3PtBr_5^-$ and 208 cm^{-1} in $^3OsBr_5^-$) to vibrational coherence impulsively induced during the ligand dissociation process. The dissociation reaction coordinate in $PtBr_6^{2-}$ has a projection on the a_1 113 cm^{-1} mode in $^3PtBr_5^-$ because its nuclear displacements can be viewed as the closure of four equatorial ligands on the coordination site vacated by the ligand. We note that although the t_{1u} doming vibration of $PtBr_6^{2-}$ (117 cm^{-1}, B3LYP), which descends to a_1 symmetry in C_{2v}, has a large projection on the umbrella-like a_1 mode (113 cm^{-1}) of $^3PtBr_5^-$, it is not observed in the resonance Raman measurements on the six-coordinate reactant species. For $^3OsBr_5^-$, the a_1 mode (217 cm^{-1}, B3LYP) involves shortening of the axial Os−Br bond as well as stretching of four equatorial Os−Br bonds, which are slightly bent toward the vacated coordination site and may be viewed similarly. Motion along the vacancy closure was predicted to begin already on a minor extension of the metal−ligand bond[19,30] and is consistent with the observation of the a_1 modes almost immediately (e.g., -7 ± 8 fs in $^3PtBr_5^-$) after reaching the Franck−Condon state. The wavepacket in $^3OsBr_5^-$ is more delocalized than that of $PtBr_6^{2-}$ because of the larger energy level spacing, and as a result, $^3OsBr_5^-$ exhibits weaker modulations in the transient absorption.

The vibrationally coherent 78 cm^{-1} mode in $^3PtBr_5^-$ exhibits a noticeable ∼30 fs time lag. This suggests that the corresponding a_1 bending motion only begins later than the a_1 umbrella motion. Although the a_1 bending motion is similar to the t_{2u} pucker vibration in the parent $PtBr_6^{2-}$ complex, the latter mode has zero projection to Franck−Condon active coordinates. In addition, the time lag is an appreciable fraction of the bending oscillatory period (427 fs), suggesting that the wave packet emerges on the product state potential surface very fast (∼30 fs) but not instantaneously. Therefore, time for relaxation of a wavepacket out of the dissociation exit channel[29] is required to observe bending motion. How then is coherent excitation of the bending mode possible? Following excitation of $PtBr_6^{2-}$ into $^1T_{2g}$, electronic relaxation via the manifold of closely lying singlet states leads to the lowest singlet-excited $^1T_{1g}$ state (guided by Raman-active modes, consistent with Kasha's rule), where the wavepacket undergoes a partial, Raman-active oscillation promoting ISC, and ultimately populates the $^3T_{1g}$ dissociative state. The wavepacket then moves on the $^3T_{1g}$ PES along the reaction coordinate dominated by the t_{1u} antisymmetric stretch toward the exit, reached without significant spreading well within 150 fs after excitation at a C_{4v} geometry of $PtBr_5^-$. In the $PtBr_5^-$ species, the first excited triplet state of ^3E character is populated because it correlates to the lowest $^3T_{1g}$ state in O_h.[18,19] When the compact wavepacket passes through the CI, it is accelerated on the steep potential slopes of the CI region, and the b_1 and b_2 splitting modes become excited. A mapping of the ground-state PES of $^3PtBr_5^-$ along the b_1 pucker and b_2 scissor motions conforms to the topology characteristic of the JT C_{4v} CI, displaying two equivalent minima separated by the ridge with two equivalent saddle points along the moat, Figure 4. The only other available b_1/b_2 combination of out-of-phase stretch and scissor does not yield this topology. Therefore, the b_1 pucker and b_2 scissor in C_{4v}, which descend to the a_1 bending and a_2 twisting in C_{2v}, dominate the gradient difference and derivative coupling vectors, respectively. As the excited-state wavepacket is directed toward the CI by b_2 scissor, which is a C_{4v} component of the Raman-active T_{2g} motion in $PtBr_6^{2-}$, one expects that following the passage through

the CI, the wavepacket continues to propagate along the b_2 ridge separating two quasi-D_{3h} ground-state minima before plummeting in one of them. It is known that the deposition of large excess energy into a vibrational mode along the reaction path suppresses the coherence in this mode due to anharmonicity.[21,29] The detection of the 78 cm^{-1} oscillations, albeit exhibiting some anharmonicity and being quickly suppressed, probably suggests that the a_1 bending component of the reaction path stores a small part of the energy, with a major part of excess energy released along a_2 twisting.

The mechanistic photochemistry of $OsBr_6^{2-}$ is similar to that of $Cr(CO)_6$ but involves the triplet manifold. Following dissociation of $OsBr_6^{2-}$, after a temporal onset of about 30 fs, the E′ wavepacket of $OsBr_5^-$ arrives to a D_{3h} geometry,[19,30] JT D_{3h} CI. A mapping of the ground-state PES of $^3OsBr_5^-$ along the available e coordinates showed that the e′ modes, corresponding to the symmetric a_1 and antisymmetric b_2 bending in C_{2v}, dominate the gradient difference and derivative coupling vectors. This is the picture similar to $Cr(CO)_5$.[19] The calculated PES is also similar to the $^1S_0$ PES of $Cr(CO)_5$, exhibiting a three-fold symmetry due to nonzero quadratic coupling with the moat that encircles the D_{3h} CI and displays equivalent C_{4v} minima separated by C_{2v} transition states, Figure 4. In $Cr(CO)_5$, the wavepacket first undergoes a partial oscillation along the a_1 bending and then descends along the b_2 bending to one of two C_{4v} product minima, where coherent motion is detected. In $^3OsBr_5^-$, coherences in either the a_1 or b_2 bending modes are not observed. A tentative explanation is that the JT-active bending vibrations of $^3OsBr_5^-$ are of low-frequency (sub-50 cm^{-1}) and expected to damp out very quickly.[21]

In conclusion, the wavepacket motion following excitation of $PtBr_6^{2-}$ and $OsBr_6^{2-}$ in water and methanol solutions was monitored using ultrafast pump−probe spectroscopy. Vibrational coherences are observed in the reaction coordinate mode that leads through several CIs as well as in the spectator modes that preserve the electronic degeneracy. Namely, the triplet ground-state products formed in less than 150 fs show coherent oscillations impulsively induced during the ligand dissociation process with the subpicosecond damping times and frequencies corresponding to spectator a_1 modes excited near the surface bottom, 113 cm^{-1} (umbrella) in $^3PtBr_5^-$ and 208 cm^{-1} (equatorial stretch) in $^3OsBr_5^-$. This observation contributes to a growing body of evidence[31] that vibrational coherence can persist in transition-metal complexes with significant excess energy in aqueous solutions. Much more interestingly, the $^3PtBr_5^-$ photoproduct displays the coherent 78 cm^{-1} a_1 bending mode, which is parallel to the gradient difference b_1 vector of the JT C_{4v} CI present in the photochemical reaction pathway. We interpret this coherence as being induced by acceleration of a compact wavepacket on the steep potential energy slopes in the vicinity of the CI. The situation for $^3PtBr_5^-$ is thus unlike that for tetrakis(dimethylamino)ethylene, where coherence is detected in the umbrella mode coupled with the CI degeneracy lifting modes.[11] The rapid loss of coherence in the normal mode parallel to the gradient difference vector is observed after the passage of the wavepacket through the CI region.

■ ASSOCIATED CONTENT

Supporting Information. Description of quantum chemical methods used and the angles in the $^3PtBr_5^-$ species. This material is available free of charge via the Internet at http://pubs.acs.org.

■ AUTHOR INFORMATION

Corresponding Author

*E-mail: atarnov@bgsu.edu. Phone: 1-(419)-372-3865. Fax:1-(419)-372-9809.

Present Addresses

†Department of Chemistry, University of Kansas, Lawrence, KS 66045, United States.

‡Department of Chemistry, Emory University, Atlanta, GA 30322, United States.

■ ACKNOWLEDGMENT

This work was supported by the NSF CAREER award (Grant CHE-0847707, A.N.T.). An allocation of computer time from the Ohio Supercomputer Center is gratefully acknowledged. Discussions with M. Olivucci, B. Dietzek, and J. M. Herbert are gratefully acknowledged.

■ REFERENCES

(1) Butler, L. J. Chemical Reaction Dynamics beyond the Born−Oppenheimer Approximation. *Annu. Rev. Phys. Chem.* **1998**, *49*, 125–171.

(2) Yarkony, D. R. Diabolical Conical Intersections. *Rev. Mod. Phys.* **1996**, *68*, 985–1013.

(3) Worth, G. A.; Cederbaum, L. S. Molecular Dynamics through a Conical Intersection. *Annu. Rev. Phys. Chem.* **2004**, *55*, 127–158.

(4) Paterson, M. J.; Bearpark, M. J.; Robb, M. A.; Blancafort, L.; Worth, G. A. Conical Intersections: A Perspective on the Computation of Spectroscopic Jahn−Teller Parameters and the Degenerate 'Intersection Space'. *Phys. Chem. Chem. Phys.* **2005**, *7*, 2100–2115.

(5) Banin, U.; Ruhman, S. Ultrafast Photodissociation of I_3^- — Coherent Photochemistry in Solution. *J. Chem. Phys.* **1993**, *98*, 4391–4403.

(6) Wang, Q.; Schoenlein, R. W.; Peteanu, L. A.; Mathies, R. A.; Shank, C. V. Vibrationally Coherent Photochemistry in the Femtosecond Primary Event of Vision. *Science* **1994**, *266*, 422–424.

(7) Vos, M. H.; Rappaport, F.; Lambry, J. C.; Breton, J.; Martin, J. L. Visualization of Coherent Nuclear Motion in a Membrane Protein by Femtosecond Spectroscopy. *Nature* **1993**, *363*, 320–325.

(8) Zhu, L.; Sage, J. T.; Champion, P. M. Observation of Coherent Reaction Dynamics in Heme-Proteins. *Science* **1994**, *266*, 629–632.

(9) Trushin, S. A.; Fuss, W.; Schmid, W. E.; Kompa, K. L. Femtosecond Dynamics and Vibrational Coherence in Gas-Phase Ultraviolet Photodecomposition of $Cr(CO)_6$. *J. Phys. Chem. A* **1998**, *102*, 4129–4137.

(10) Trushin, S. A.; Fuss, W.; Schmid, W. E. Conical Intersections, Pseudorotation and Coherent Oscillations in Ultrafast Photodissociation of Group-6 Metal Hexacarbonyls. *Chem. Phys.* **2000**, *259*, 313–330.

(11) Sorgues, S.; Mestdagh, J. M.; Visticot, J. P.; Soep, B. Wave Packet Movements Near the Conical Intersection between Two excited Potential Surfaces May Create Observable Molecular Oscillations. *Phys. Rev. Lett.* **2003**, *91*, 103001.

(12) Trushin, S. A.; Kosma, K.; Fuss, W.; Schmid, W. E. Wavelength-Independent Ultrafast Dynamics and Coherent Oscillation of a Metal−Carbon Stretch Vibration in Photodissociation of $Cr(CO)_6$ in the Region of 270−345 nm. *Chem. Phys.* **2008**, *347*, 309–323.

(13) Wurzer, A. J.; Wilhelm, T.; Piel, J.; Riedle, E. Comprehensive Measurement of the S_1 Azulene Relaxation Dynamics and Observation of Vibrational Wavepacket Motion. *Chem. Phys. Lett.* **1999**, *299*, 296–302.

(14) Farrow, D. A.; Qian, W.; Smith, E. R.; Ferro, A. A.; Jonas, D. M. Polarized Pump−Probe Measurements of Electronic Motion via a Conical Intersection. *J. Chem. Phys.* **2008**, *128*, 144510.

(15) Bixon, M.; Jortner, J. Vibrational Coherence in Nonadiabatic Dynamics. *J. Chem. Phys.* **1997**, *107*, 1470–1482.

(16) Jorgensen, C. K. Electron Transfer Spectra of Hexahalide Complexes. *Mol. Phys.* **1959**, *2*, 309–332.

(17) Balzani, V.; Manfrin, M. F.; Moggi, L. Photochemistry of Coordination Compounds. 16. Hexabromoplatinate(IV) and Hexaiodoplatinate(IV) Ions. *Inorg. Chem.* **1967**, *6*, 354–358.

(18) Pollak, C.; Rosa, A.; Baerends, E. J. Cr−CO Photodissociation in $Cr(CO)_6$: Reassessment of the Role of Ligand-Field Excited States in the Photochemical Dissociation of Metal−Ligand Bonds. *J. Am. Chem. Soc.* **1997**, *119*, 7324–7329.

(19) Paterson, M. J.; Hunt, P. A.; Robb, M. A.; Takahashi, O. Non-Adiabatic Direct Dynamics Study of Chromium Hexacarbonyl Photodissociation. *J. Phys. Chem. A* **2002**, *106*, 10494–10504.

(20) Voskresenska, V.; Wilson, R. M.; Panov, M.; Tarnovsky, A. N.; Krause, J. A.; Vyas, S.; Winter, A. H.; Hadad, C. M. Photoaffinity Labeling via Nitrenium Ion Chemistry: Protonation of the Nitrene Derived from 4-Amino-3-nitrophenyl Azide to Afford Reactive Nitrenium Ion Pairs. *J. Am. Chem. Soc.* **2009**, *131*, 11535–11547.

(21) Vöhringer, P.; Westervelt, R. A.; Yang, T. S.; Arnett, D. C.; Feldstein, M. J.; Scherer, N. F. Solvent and Frequency Dependence of Vibrational Dephasing on Femtosecond Time-Scales. *J. Raman Spectrosc.* **1995**, *26*, 535–551.

(22) Pollard, W. T.; Dexheimer, S. L.; Wang, Q.; Peteanu, L. A.; Shank, C. V.; Mathies, R. A. Theory of Dynamic Absorption Spectroscopy of Nonstationary States. 4. Application to 12-fs Resonant Impulsive Raman Spectroscopy of Bacteriorhodopsin. *J. Phys. Chem.* **1992**, *96*, 6147–6158.

(23) Elsäesser, T.; Kaiser, W. Vibrational and Vibronic Relaxation of Large Polyatomic Molecules in Liquids. *Annu. Rev. Phys. Chem.* **1991**, *42*, 83–107.

(24) Gawelda, W.; Cannizzo, A.; Pham, V. T.; van Mourik, F.; Bressler, C.; Chergui, M. Ultrafast Nonadiabatic Dynamics of $[Fe^{II}(bpy)_3]^{2+}$ in Solution. *J. Am. Chem. Soc.* **2007**, *129*, 8199–8206.

(25) Kovalenko, S. A.; Dobryakov, A. L.; Farztdinov, V. Detecting Electronic Coherence in Excited-State Electron Transfer in Fluorinated Benzenes. *Phys. Rev. Lett.* **2006**, *96*, 068301.

(26) Ostroumov, E.; Muller, M. G.; Marian, C. M.; Kleinschmidt, M.; Holzwarth, A. R. Electronic Coherence Provides a Direct Proof for Energy-Level Crossing in Photoexcited Lutein and Beta-Carotene. *Phys. Rev. Lett.* **2009**, *103*, 108302.

(27) Bradforth, S. E.; Jimenez, R.; van Mourik, F.; van Grondelle, R.; Fleming, G. R. Excitation Transfer in the Core Light-Harvesting Complex (LH-1) of Rhodobacter-Sphaeroides — An Ultrafast Fluorescence Depolarization and Annihilation Study. *J. Phys. Chem.* **1995**, *99*, 16179–16191.

(28) Arnett, D. C.; Vöhringer, P.; Scherer, N. F. Excitation Dephasing, Product Formation, and Vibrational Coherence in an Intervalence Charge-Transfer Reaction. *J. Am. Chem. Soc.* **1995**, *117*, 12262–12272.

(29) Jean, J. M.; Fleming, G. R. Competition between Energy and Phase Relaxation in Electronic Curve Crossing Processes. *J. Chem. Phys.* **1995**, *103*, 2092–2101.

(30) Worth, G. A.; Welch, G.; Paterson, M. J. Wavepacket Dynamics Study of $Cr(CO)_5$ after Formation by Photodissociation: Relaxation through an $(E \oplus A) \otimes e$ Jahn−Teller Conical Intersection. *Mol. Phys.* **2006**, *104*, 1095–1105.

(31) Consani, C.; Premont-Schwarz, M.; Elnahhas, A.; Bressler, C.; van Mourik, F.; Cannizzo, A.; Chergui, M. Vibrational Coherences and Relaxation in the High-Spin State of Aqueous $[Fe^{II}(bpy)_3]^{2+}$. *Angew. Chem., Int. Ed.* **2009**, *48*, 7184–7187.